

# Tailor-structured skeletal Pt catalysts employed in a monolithic electropromoted reactor

A. Hammad · S. Souentie · S. Balomenou ·  
D. Tsiplakides · J. C. Figueroa · C. Cavalca ·  
C. J. Pereira · C. G. Vayenas

Received: 22 November 2007 / Revised: 26 February 2008 / Accepted: 26 February 2008 / Published online: 11 March 2008  
© Springer Science+Business Media B.V. 2008

**Abstract** The performance of a monolithic electropromoted reactor was investigated under high gas flow rates, for the oxidation of ethylene utilizing thin (40 nm) tailor-structured highly porous skeletal Pt catalyst-electrodes coated on  $Y_2O_3$ -stabilized- $ZrO_2$  (YSZ). Electrochemical enhancement was observed at gas flow rates as high as  $25\text{ L min}^{-1}$  and mean gas residence times as low as 0.15 s. This is a promising step for the practical utilization of the electrochemical promotion of catalysis. An interesting feature of the skeletal Pt catalyst-electrodes is the appearance of a sharp rate maximum upon anodic current interruption which appears to be related to their dendritic structure and enhanced capacity for promoter storage.

**Keywords** Electrochemical promotion · Monolithic electrochemically promoted reactor · Ethylene oxidation · MEPR · Skeletal Pt electrodes ·  $Y_2O_3$ -stabilized- $ZrO_2$

## 1 Introduction

The electrochemical promotion of catalysis (non-Faradaic electrochemical modification of catalytic activity, NEMCA

effect) refers to the very pronounced and reversible changes in the catalytic properties of conductive catalysts deposited on solid electrolytes caused by application of small electrical currents or potentials [1–18]. There exist shorter [4, 6, 14, 15] as well as more detailed recent reviews [3, 5] describing the phenomenology, limits and molecular origin of the phenomenon. Electrochemical promotion has been studied extensively for more than 15 years almost exclusively in research laboratories but there is also a strong industrial interest and involvement aiming at commercialization. However, several aspects have to be addressed before the practical exploitation of electrochemical promotion.

A major thrust was realized through the confirmation of the feasibility of electropromotion of thin sputtered metal films [19, 20] and the development of the monolithic electrochemically promoted reactor, MEPR [4, 20]. Sputtered metal films on un-treated YSZ surfaces, with a thickness of 40–50 nm, were reported to have a metal dispersion higher than 10–20% [20], which is comparable to that of state-of-the-art conventional supported catalysts. The performance of these films is remarkable not only in terms of electrochemical promotion efficiency but also in reference to long-term stability and endurance. Following the advances in nanotechnology, alternative coating methods such as chemical vapor deposition (CVD) or electrostatic spray deposition (ESD) may be also taken under consideration for electrochemical promotion applications.

On the other hand, the recently developed MEP reactor [20] provides a practical structured electrochemically promoted reactor which allows, in principle, the transition from laboratory studies to practical applications. The electropromoted reactor has already been evaluated successfully for hydrocarbon oxidation and NO reduction by  $C_2H_4$  in the presence of  $O_2$  using both conventional thick

A. Hammad · S. Souentie · C. G. Vayenas  
Department of Chemical Engineering, University of Patras,  
26504 Patras, Greece

S. Balomenou (✉) · D. Tsiplakides  
CPERI/CERTH, 6th km Charilaou-Thermi Rd., 57001  
Thessaloniki, Greece  
e-mail: stellab@cperi.certh.gr

J. C. Figueroa · C. Cavalca · C. J. Pereira  
DuPont Company, Central Research & Development MS&E,  
Wilmington, DE 19880, USA

films and thin sputtered noble metal electrodes [4, 20–22]. It was also tested for the treatment of automotive exhaust gas of a real diesel engine [22] demonstrating excellent mechanical and thermal stability after prolonged operation.

In the present work we explore the performance of an electropromoted reactor under high gas flow rates (as high as  $25 \text{ dm}^3 \text{ min}^{-1}$  or  $25 \text{ L min}^{-1}$ ) for the ethylene oxidation reaction utilizing tailor-structured skeletal Pt catalyst-electrodes prepared by vapor deposition. The reactor volume was  $125 \text{ cm}^3$  ( $5 \times 5 \times 5 \text{ cm}^3$ ), so that, these flow rates, correspond to a space time of 0.3 s, and at  $300 \text{ }^\circ\text{C}$  to a residence time of 0.15 s and a gas velocity of  $0.34 \text{ m s}^{-1}$  in the rectangular ducts (channels) of the reactor. Thus the hourly space velocity is up to  $1.2 \times 10^4 \text{ h}^{-1}$ , which is comparable to the space velocities in commercial reactors and the maximum ones reported in the electrochemical promotion literature.

## 2 Experimental

### 2.1 MEP reactor design and construction

The MEP reactor can be considered as a hybrid between a classical monolithic honeycomb reactor and a planar solid oxide fuel cell [23]. The reactor concept and design (Fig. 1) has been described in detail elsewhere [4, 20, 21]. In brief, the core of the MEPR is a ceramic casing, made of machinable glass ceramic (Macor<sup>®</sup>™, [20, 21]). The

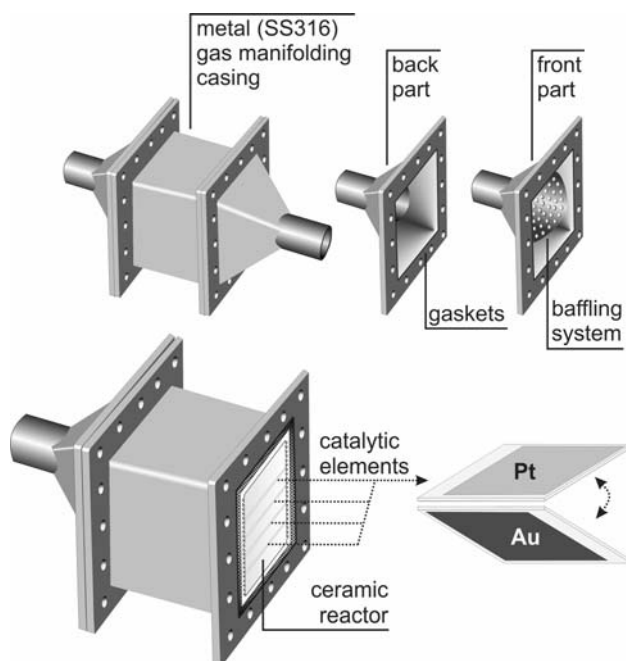


**Fig. 1** Schematic of the assembled monolithic electropromoted reactor (MEPR)

internal faces of the two opposing reactor walls have appropriately machined parallel grooves where a number of solid electrolyte plates are inserted. These surfaces are also used to create the two necessary current collectors, one establishing electrical contact with all catalyst films deposited on the top side of the plates, while the other current collector establishes electrical contact with all catalyst films deposited on the bottom side of the plates. In this way, a significant practical simplification is realized as both the top and bottom catalyst films can be electrochemically promoted (with reverse polarity) via only two external connecting wires. The reactor is enclosed in a suitable metal casing of stainless steel with a baffling system at the gas entrance aiming to achieve as uniform a gas flow distribution as possible at the gas entrance. The baffle geometry was presented in [20]. Vermiculite insulating material was placed between the ceramic reactor walls and the metal gas manifold casing [20].

The MEP reactor is a simple device that permits easy practical utilization of electrochemical promotion. It accomplishes an efficient and compact reactor design, which can be assembled and dismantled at will, has only two external connecting wires and its catalytic plates can be replaced whenever necessary. It exhibits excellent mechanical and thermal stability enabling its use under harsh environments, such as in a car engine exhaust. Furthermore it is possible to use one of the plates as a gas-sensor element and utilize the potential signal generated by this element to dynamically control the current or potential applied to the electropromoted catalytic plates. The MEP reactor can, conceptually, be scaled-up (or scaled-down) following a stack design and can, in principle, be used for many practical applications in exhaust treatment units and in chemical destruction or synthesis processes.

### 2.2 YSZ solid electrolyte plates and catalysts preparation

The solid electrolyte plates, CERAFLEX 8Y, had a thickness of 0.5 mm and dimensions of  $50 \text{ mm} \times 50 \text{ mm}$ . They were made of yttria-stabilized-zirconia (YSZ, 8 mol%  $\text{Y}_2\text{O}_3$ , 13.8 wt%) with a resulting molar composition  $\text{Zr}_{0.913}\text{Y}_{0.087}\text{O}_{1.957}$ .

The Pt catalyst films were prepared by a three step procedure according to DuPont owned US Patent 5,993,979 (1999) [24]:

*Step 1:* The catalytic element of choice (Pt) is co-deposited on the YSZ substrate together with a leachable material (Al) using vapor deposition technique. Thickness and elemental control is achieved by the balance between power delivered to the given target (Pt or Al) and residence time of the support under the given target.

*Step 2:* The formed layer is homogenized and stabilized by thermal treatment.

*Step 3:* After the layer comprising the metal (Pt)/leachable material (Al) composite is in place and heat treated, activation is realized through the preferential leaching out of Al by immersion in a NaOH aqueous solution.

This procedure provides highly porous skeletal column coatings comprising a well adhered columnar structure having both inter-column and intra-column porosity. A scanning electron micrograph of such catalyst-electrodes is shown in Fig. 2. Their texture is reminiscent of Raney Ni, which is actually prepared in a similar manner. The thickness of these highly porous Pt films was roughly 40 nm. Judging from the slow rate response ( $\tau \approx 10$  min) observed with imposed anodic currents as high as 120 mA it becomes clear that their surface area is quite high. Thus using  $N_G = I \cdot \tau / 2F$  [3] to estimate their active surface area  $N_G$  one finds  $N_G \approx 3.7 \times 10^{-4}$  mol Pt which is of the same order of magnitude as the total mass of the Pt films. So the metal dispersion must be at least as high as that (10–40%) obtained with sputter-coated Pt films of comparable thickness [20]. Typical Au paste electrodes were deposited on the opposite side of the YSZ plates and used as counter-electrodes.

### 2.3 MEPR operation

The MEP reactor was placed in a tubular furnace and its temperature was measured and controlled by two type K (chromel-alumel) thermocouples embedded in the metal casing at a distance of 1 mm from the gas entrance and exit. In order to accomplish uniform temperature in the reactor under high reactant flow rates, a pre-heater was

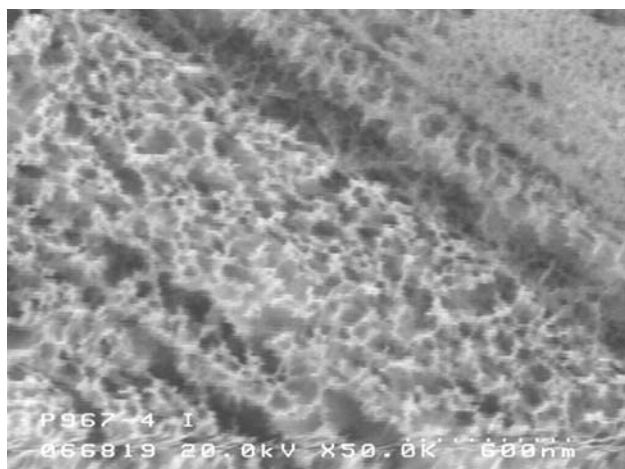


**Fig. 2** SEM micrographs (top view) of the highly porous Pt skeletal coatings on YSZ

placed just in front of the furnace entrance. The feed gas composition and total flow rate,  $F_v$ , was controlled by four mass flowmeters (Brooks smart mass flow and controller B5878). Reactants were Messer-Griesheim certified standards of  $C_2H_4$  in He and  $O_2$  in He. The total flow rate and inlet gas composition was adjusted by the use of pure (99.99%) He feed through the fourth flowmeter. Products were analyzed via an IR  $CO_2$  analyzer (Rosemount Binol 100). Constant currents and potentials were applied using an AMEL 553 galvanostat–potentiostat.

In the present experiments four (4) Pt/YSZ/Au elements (size  $5 \times 5$  cm<sup>2</sup>) were placed in the MEP reactor with equal spacing of 1 cm (Fig. 1).

As in previous studies [1, 3] the magnitude of the electrochemical promotion effect is commonly described by two parameters. The first one is the Faradaic efficiency,  $\Lambda$ , defined from:

$$\Lambda = \frac{r - r_o}{(I/2F)} = \frac{\Delta r}{(I/2F)} \quad (1)$$

where  $r_o$  is the open-circuit (unpromoted) rate (expressed in mol O s<sup>-1</sup>),  $r$  is the electropromoted rate ( $=r_o + \Delta r$ ),  $I$  is the applied current and thus, from Faraday's law,  $I/2F$  is the rate of supply of  $O^{2-}$  to the catalyst surface. The nature of these spillover  $O^{\delta-}$  ions, which are distinct from chemisorbed O formed by gaseous adsorption, has been studied with numerous electrochemical, catalytic and surface science techniques [3–6, 11–13]. Typically  $|\Lambda|$  varies from 10 to  $10^5$  depending on the reaction, the catalyst material and morphology, the type of solid electrolyte and the operating temperature [3–6, 11–13].

The second parameter describing the magnitude of electrochemical promotion is the rate enhancement ratio,  $\rho$ , defined by:

$$\rho = r/r_o \quad (2)$$

Typically  $\rho$  is of the order 2–100 [1–3] but values as high as 1,200 have been recently reported [25, 26].

In practical electrochemically promoted units [20–22] aiming at near complete reactant conversion a third important parameter is the effective rate enhancement ratio,  $\rho_c$ , defined from:

$$\rho_c = \rho/\rho_{\max} \quad (3)$$

where  $\rho_{\max}$  corresponds to the maximum  $\rho$  value allowed from thermodynamics, i.e. corresponding to equilibrium conversion. Thus in the present case of  $C_2H_4$  oxidation  $\rho_{\max}$  corresponds to near complete conversion of ethylene.

## 3 Results and discussion

A typical potentiostatic transient, i.e., reaction rate and current response to a potential step, is presented in Fig. 3.

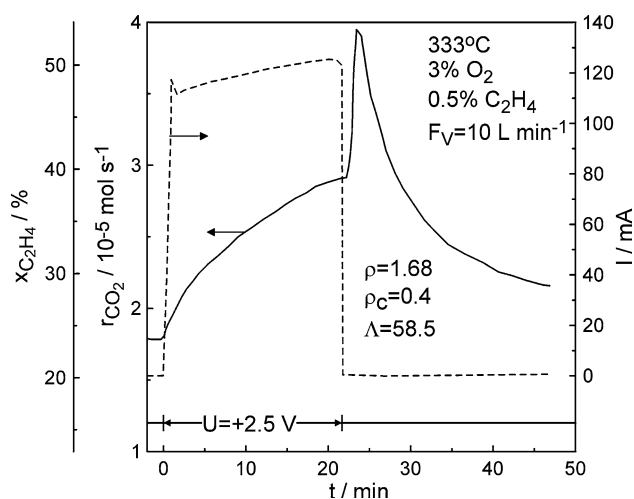


**Fig. 3** Potentiostatic transient: reaction rate and current response to a potential step of 2.5 V applied to the Pt catalyst elements (inlet conditions:  $p_{\text{O}_2} = 3$  kPa,  $p_{\text{C}_2\text{H}_4} = 0.5$  kPa,  $F_v = 10$  L  $\text{min}^{-1}$ ,  $T = 333$  °C)

The inlet ethylene and oxygen partial pressures are  $p_{\text{C}_2\text{H}_4} = 0.5$  kPa and  $p_{\text{O}_2} = 3$  kPa and the applied potential is 2.5 V, leading to a current of the order of 120 mA and thus, accounting for the total superficial surface area of the Pt films ( $4 \times 25$  cm<sup>2</sup>), to a current density of  $\sim 1.2$  mA cm<sup>-2</sup>. This is higher than the current densities obtained under similar conditions with Pt paste films or sputter-coated films and reflects the very high three-phase-boundary (tpb) length of the skeletal electrodes. As shown in Fig. 3, upon potential application the system presents a typical behavior for an electrochemically promoted catalyst: the reaction rate gradually increases, approaching a new steady-state value after 20 min which is 68% higher than the open circuit rate ( $\rho = 1.68$ ) and 58.5 times higher than the rate of oxygen ions supply,  $I/2F$ , from the solid electrolyte to the catalyst, i.e. the Faradaic efficiency,  $\Lambda$ , equals 58.5. The conversion of  $\text{C}_2\text{H}_4$  increases from 23% to 39% and since complete conversion corresponds to  $\rho_{\text{max}} = 4.3$  it follows that the effective rate enhancement ratio,  $\rho_c$ , equals  $1.68/4.3$ , i.e. 0.4.

We have used only potentiostatic transients because the applied potential is controlled precisely and cannot exceed the upper limit of 3.5 V, above which it is known that electrolysis of the YSZ plates may start taking place. In the galvanostatic operation one can easily exceed this limit if the applied current is too high. In any event as shown in Fig. 3 the current reaches quickly a nearly constant value, so that the usual analysis of determining  $\tau$  and thus the anode surface area can still be applied with reasonable accuracy.

A striking feature of Fig. 3, not observed in previous NEMCA studies, is that potential interruption leads to an unexpected sharp reaction rate peak followed by a

relatively slow decrease towards a value which is about 1.2 times higher than the initial (before potential application) open-circuit rate. While an enhanced open-circuit rate following anodic polarization is common in several NEMCA studies [3, 27, 29], termed “permanent NEMCA”, and corresponding to an active metastable state of the catalyst surface, this type of peak is observed for the first time, at least of that magnitude. The observed phenomenon deserves much closer investigation. It is likely that it can be attributed to the dendritic structure of Pt skeletal electrodes (Fig. 2) and the concomitant ease of trapping of backspillover ions in isolated branches of these dendrites, i.e. in positions where they can affect via repulsive interactions and thus activate only few neighboring gas-supplied oxygen atoms. After current interruption these backspillover ions partly react with the fuel and partly migrate towards the electrolyte following their electrochemical potential gradient. During this back-migration they reach regions of thicker dendritic branches, where each of them can activate many more surrounding gas-supplied oxygen atoms. Eventually, as oxygen ions are not further supplied to the surface the rate decreases with a characteristic slow rate, as in every NEMCA transient.

A similar behaviour, that is activation of catalyst after current interruption, was observed by Jaccoud et al. [28, 29] for a Pt thick (1  $\mu\text{m}$ ) film deposited on YSZ. The phenomenon was present only after prolonged polarization and was attributed to oxygen storage occurring at a location hidden from the gas phase (“hidden promoter” model) at the Pt/YSZ interface. Due to slow diffusion, the promoting effect of these hidden oxygen species appears hours after current interruption resulting in a hump, rather than a peak, in the reaction rate during depolarization. The interpretation of the peak observed here with the Pt skeletal electrodes, is conceptually similar to that of Jaccoud et al. [28, 29], since the remote and isolated fine branches of the dendritic structure may also serve as a location for promoter storage.

The effect of applied potential on the  $\text{CO}_2$  formation rate at fixed inlet gas composition (0.5%  $\text{C}_2\text{H}_4$ , 3%  $\text{O}_2$ ) under steady-state conditions is presented in Fig. 4. In agreement with previous NEMCA studies of ethylene oxidation on Pt/YSZ, the rate exhibits electrophobic behaviour, that is the rate increases with potential, reaching a plateau at 2.5 V where the ethylene conversion is about 85%. At this point, the rate enhancement ratio equals 2.2 and the effective rate enhancement ratio,  $\rho_c (= \rho/\rho_{\text{max}}$ , where  $\rho_{\text{max}}$  is the maximum possible  $\rho$  value at full conversion) equals 0.88. The small deviation from full conversion can be attributed to the gas by-pass through the bottom channel of the MEP reactor [20]. In this channel the gas mixture encounters only the Au counter electrode. If this electrode were totally inactive for  $\text{C}_2\text{H}_4$  oxidation and

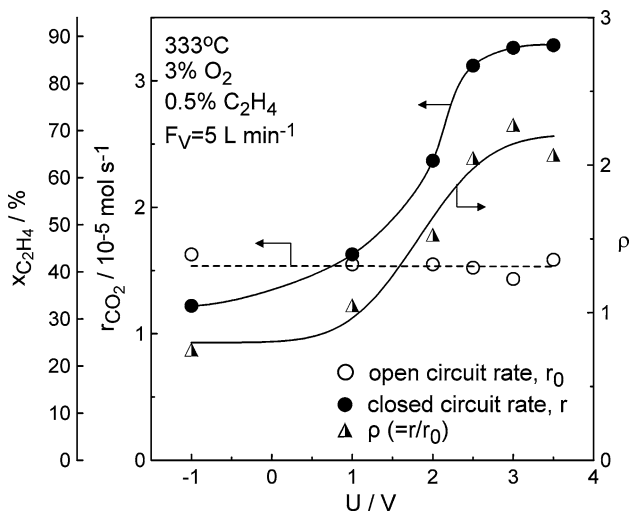


**Fig. 4** Effect of applied potential on the open-circuit and closed-circuit catalytic rate and on the rate enhancement ratio  $\rho$  (inlet conditions:  $p_{O_2} = 3$  kPa,  $p_{C_2H_4} = 0.5$  kPa,  $F_v = 5$  L min<sup>-1</sup>),  $T = 333$  °C

if the flow distribution between the five channels was exactly uniform, then  $\rho_c$  could not exceed 0.8 with the present reactor design. The fact that  $\rho_c$  reaches the value of 0.88 suggests that the actual flow through bottom (and also top) channel is smaller than through the other three channels and thus suggests the need for improvements of the baffling gas distribution system. In any case, the electro-promotion of this very active catalyst (open-circuit conversion 40%) to almost full conversion shows the excellent capability of the MEP reactor for the electro-promotion of already quite effective catalysts.

It should be noted that, under the relatively low flow rate conditions of Fig. 4, the effect was reversible, i.e. no permanent NEMCA behaviour was observed. This is different from the behaviour at higher flow rates, as for example in Fig. 3, where the open-circuit rate after current interruption was 20–30% higher than the initial one. Permanent NEMCA behaviour was always preceded by the sharp rate peak, already discussed above.

The effect of gas flow rate at constant feed composition on both the open-circuit and the electro-promoted catalytic rate is depicted on Fig. 5. The open circuit rate is continuously increasing with flow rate, indicating at first mass transfer limitations even at 25 L min<sup>-1</sup>. However, the calculated mass transfer controlled rate lies well above the measured catalytic rate, even under potential application. This is the case even if one assumes that the thickness of the boundary layer in the rectangular channels (ducts) equals the spacing,  $\ell (= 1$  cm) between the plates which is a very conservative estimate. The thus computed mass transport controlled rate per unit superficial catalyst surface area is then given by [30]

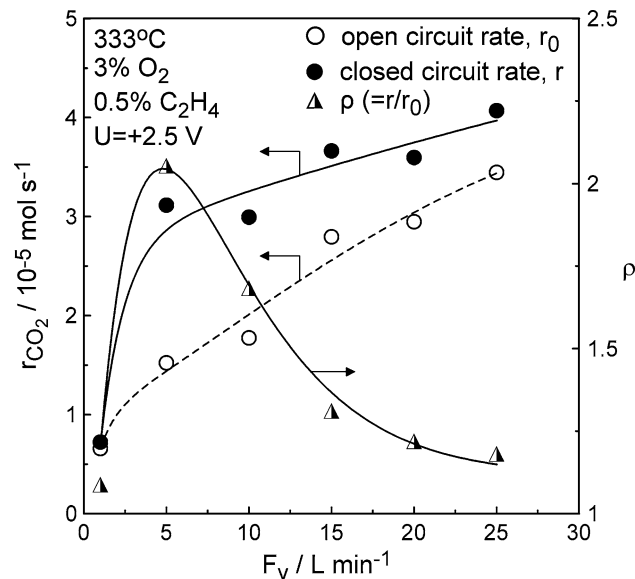


**Fig. 5** Effect of gas flow rate on the open-circuit and under potential catalytic rate and on the rate enhancement ratio  $\rho$  and effective rate enhancement ratio  $\rho_c$  (inlet conditions:  $p_{O_2} = 3$  kPa,  $p_{C_2H_4} = 0.5$  kPa),  $T = 333$  °C

$$r_{mc} = k_g [C_2H_4] = (D_{C_2H_4} / \ell) [C_2H_4] \tag{4}$$

where  $[C_2H_4]$  is the average gaseous concentration of  $C_2H_4$ ,  $D_{C_2H_4} (\sim 0.1$  cm<sup>2</sup> s<sup>-1</sup>) is the diffusivity of  $C_2H_4$  in the reacting mixture and  $k_g$  is the mass transfer coefficient (cm s<sup>-1</sup>).

Thus the observed increase in the rate with flow rate is due to the decreasing conversion of  $C_2H_4$  since the experiments were performed at fixed inlet gas composition. Thus the conversion of  $C_2H_4$  decreases from 95% at 1 L min<sup>-1</sup> to 20% at 25 L min<sup>-1</sup>, thus the average  $p_{C_2H_4}$  value in the reactor increases by more than a factor of ten (from  $5 \times 10^{-2}$  kPa to 0.45 kPa) as the flow rate increases from 1 to 25 L min<sup>-1</sup>. Thus the observed rate increase with flow rate is simply due to the increasing average  $p_{C_2H_4}$  value with increasing flow rate. It is noteworthy that the application of constant potential enhances the catalyst activity over the whole range of operating flow rates, with  $\Lambda$  ranging from 110 down to 30 as flow rate was increased from 5 to 25 L min<sup>-1</sup> (Fig. 6). As already noted, at the lowest operating flow rate (1 L min<sup>-1</sup>) where the minimum  $\Lambda$  and  $\rho$  values were measured, correspond to full conversion of ethylene under potential application (effective rate enhancement  $\rho_c \approx 100\%$ , Fig. 5). Thus obviously there can be no electro-promotion at near complete reactant conversion.

The fact that electrochemical promotion can be induced on those very active Pt-catalysts at flow rates as high as 25 L min<sup>-1</sup>, corresponding mean gas residence times of 0.15 s,  $(= (V/F_v)(T_0/T))$  where  $T_0$  and  $T$  are the feed and

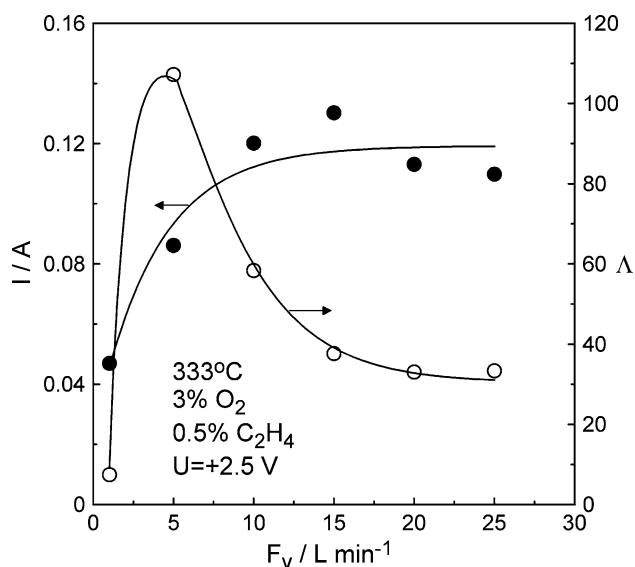


**Fig. 6** Effect of gas flow rate on the current,  $I_{wc}$ , and the Faradaic efficiency  $\Lambda$ . (inlet conditions:  $p_{O_2} = 3 \text{ kPa}$ ,  $p_{C_2H_4} = 0.5 \text{ kPa}$ ,  $T = 333 \text{ }^\circ\text{C}$ )

mean reactor temperatures respectively and  $V$  is the reactor volume) thus to hourly reactor space velocities of up to  $1.2 \times 10^4 \text{ h}^{-1}$ , is reported for the first time and appears quite promising for practical applications of EP.

#### 4 Conclusions

Thin (40 nm) skeletal-Pt films deposited on YSZ can be electropromoted in MEP reactors. An interesting feature of these films, not observed with other electropromoted catalysts, is the appearance of a sharp peak in the reaction rate upon current interruption. This phenomenon, which is worth further investigation, may be due to the ease of trapping of backspillover promoting ions in isolated branches of the dendritic structure of Pt skeletal electrodes and can be correlated to oxygen storage occurring at a location hidden from the gas phase (“hidden promoter” model) at the Pt/YSZ interface [28, 29].

On the practical side, the MEP reactor was successfully operated and electrochemical promotion was induced on the very active skeletal-Pt-catalysts at flow rates as high as  $25 \text{ L min}^{-1}$ , mean gas residence times of 0.15 s and reactor space velocities up to  $1.2 \times 10^4 \text{ h}^{-1}$ . This shows the strong potential of MEP reactors for practical applications, such as exhaust treatment units and chemical synthesis or destruction processes.

#### References

- Vayenas CG, Bebelis S, Ladas S (1990) *Nature* 343:625
- Pritchard J (1990) *Nature* 343:592
- Vayenas CG, Bebelis S, Pliangos C, Brosda S, Tsiplakides D (2001) *Electrochemical activation of catalysis: promotion, electrochemical promotion and metal-support interactions*. Kluwer Academic/Plenum Publishers, New York
- Tsiplakides D, Balomenou S, Katsaounis A, Archonta D, Koutsodontis C, Vayenas CG (2005) *Catal Today* 100:133
- Vayenas CG, Jaksic MM, Bebelis S, Neophytides SG (1996) In: Bockris JOM, Conway BE, White RE (eds) *Modern aspects of electrochemistry*, vol 29. Kluwer Academic/Plenum Publishers, New York
- Wieckowski A, Savinova E, Vayenas CG (eds) (2003) *Catalysis and electrocatalysis at nanoparticles*. Marcel Dekker, New York
- Lambert RM, Williams F, Palermo A, Tikhov MS (2000) *Top Catal* 13:91
- Foti G, Wodiunig S, Comninellis C (2000) *Curr Top Electrochem* 7:1
- Cavalca CA, Haller GL (1998) *J Catal* 177:389
- Ploense L, Salazar M, Gurau B, Smotkin ES (1997) *J Am Chem Soc* 119:11550
- Vernoux P, Gaillard F, Bultel L, Siebert E, Primet M (2002) *J Catal* 208:412
- Metcalfe I (2001) *J Catal* 199:247
- Sanchez C, Leiva E (2003) In: Vielstich W, Gasteiger H, Lamm A (eds) *Handbook of fuel cells: fundamentals, technology and applications*, vol 2. Wiley, England
- Vayenas CG, Bebelis S, Neophytides S, Yentekakis IV (1989) *Appl Phys A-Matter* 49:95
- Lintz H-G, Vayenas CG (1989) *Angew Chem Int Ed* 28:708
- Nicole J, Tsiplakides D, Pliangos C, Verykios XE, Comninellis C, Vayenas CG (2001) *J Catal* 204:23
- Riess I, Vayenas CG (2003) *Solid State Ionics* 159:313
- Dorado F, Lucas-Consuegra Ad, Jimenez C, Valverde JL (2007) *Appl Catal A-Gen* 321:86
- Baranova EA, Thursfield A, Brosda S, Foti G, Comninellis C, Vayenas CG (2005) *J Electrochem Soc* 152:E40
- Balomenou S, Tsiplakides D, Katsaounis A, Thiemann-Handler S, Cramer B, Foti G, Comninellis C, Vayenas CG (2004) *Appl Catal B-Environ* 52:181
- Balomenou SP, Tsiplakides D, Katsaounis A, Brosda S, Hammad A, Foti G, Comninellis C, Thiemann-Handler S, Cramer B, Vayenas CG (2006) *Solid State Ionics* 177:2199
- Balomenou S, Tsiplakides D, Vayenas C, Poulston S, Houel V, Collier P, Konstandopoulos A, Agrafiotis C (2007) *Top Catal* 44: 481
- Michaels JN, Vayenas CG, Hegedus LL (1986) *J Electrochem Soc* 133:522
- Figueroa JC, Mattson RH (1999) US Patent 5,993,979
- Kotsionopoulos N, Bebelis S (2005) *J Appl Electrochem* 35:1253
- Kokkofitis C, Karagiannakis G, Zisekas S, Stoukides M (2005) *J Catal* 234:476
- Nicole J, Tsiplakides D, Wodiunig S, Comninellis C (1997) *J Electrochem Soc* 144:L312
- Jaccoud A (2007) PhD Thesis, EPFL, Lausanne, Switzerland
- Jaccoud A, Foti G, Comninellis C (2006) *Electrochim Acta* 51: 1264
- Carberry JJ (1976) *Chemical and catalytic reaction engineering*. McGraw Hill, New York